2018

Wave farms grid code compliance in isolated small power systems

I. VILLALBA, M. BLANCO, J.I. PÉREZ-DÍAZ, D. FERNÁNDEZ, F. DÍAZ, M. LAFOZ

DOI: https://doi.org/10.1049/iet-rpg.2018.5351

IET Research Journals

Submission Template for IET Research Journal Papers

IET Journals
The Institution of Engineering and Technology

Wave farms grid code compliance in isolated small power systems

ISSN 1751-8644
doi: 0000000000
www.ietdl.org

Isabel Villalba[1], Marcos Blanco[2], Juan I Pérez-Díaz[3],Daniel Fernández[3], Felipe Díaz[1], Marcos Lafoz[2]*

[1] University Institute for Intelligent Systems and Numerical Applications in Engineering, University of Las Palmas de Gran Canaria, Edificio Central del Parque Tecnológico, Campus de Tafira, 35017, Las Palmas de Gran Canaria, Spain
[2] Unit of Electric Power Systems, CIEMAT,Av. Complutense, 40,28040 Madrid (Spain)
[3] E.T.S.I.C.C.P. Universidad Politécnica de Madrid,Calle del Prof. Aranguren, 3, 28040 Madrid (Spain)
** E-mail: isabel.villalba101@alu.ulpgc.es*

Abstract: Wave energy is one of the electric generation options based on renewable energies, especially suitable for islands due to the energy resource availability and the higher energy cost of energy in its electric grids. The oscillating nature of the wave resource is prone to produce negative impacts in these electric grids when considering scenarios of high penetration of wave energy generation. This paper analyses the impact of wave energy generation on the power system frequency for the particular case study of Tenerife Island (Spain). Then, hourly data related to sea states in Tenerife, during a whole year, will be provided to generate an electric power profile, based on a model of a wave energy farm with a specific wave converter type. A previously developed dynamic simulation model of the Tenerife transmission network will be fed with these power profiles and the hourly electric generation and consumption profiles to analyse the system frequency. A complete set of analysis during the whole year will be accomplished in order to determine the number of over-frequency events according to the grid codes. Finally, some corrective measures will be proposed as conclusions, e.g. energy storage devices, as the most reliable solution to mitigate frequency deviations.

1 Introduction

The renewable resource of wave energy has already demonstrated to have a great potential, estimating a power around some of TW available [1]. During the last two decades many technological developments have contributed to increase its Technology Readiness Level (TRL). Although it can still be considered to be in a non-commercial stage, due to the lack of a specific market and regulation, many prototypes and power plants (based on a variety of working principles) are being deployed and tested all over the world. The sector of the ocean energies awaken special interest in in the areas with oceanic potential, or where the cost of the electric energy is high, due to the cost of fuel and operational cost are high, which is the case of islands [2][3].

In this particular paper, Wave Energy Converters (WECs), devices for the conversion of the energy content of the waves into electricity, are considered. There exist different types of WEC, namely: oscillating wave surge converters, oscillating water columns, overtopping devices, attenuators, point absorbers, or submerged pressure differential devices [4][5].

One of the main issues of the wave energy today is the quality of the power injected into the grid [6], specially due to the oscillation of the power supplied to the electric grids [7][8], which in turn is due to the oscillating nature of the waves. The period of those power fluctuations are in the range of 5s to 25 s, affecting mainly to frequency variations [9] and voltage distortions such as flicker [10] and harmonics [11], and being more acute in weak and isolated grids, which is the case of islands, where the system inertia is low.

The impacts produced on the system frequency of a high penetration of renewable power generation (wind and photovoltaic) have been widely documented both in interconnected and isolated power systems [12][13][14][15][16][17]. However, to the authors knowledge the impact on the system frequency caused by wave power generation has so far been studied only in [9]. In [9] the impact of wave power generation on the frequency of Tenerife power system was preliminarily analysed in a reduced number of sea states and scenarios of power system operation (peak and off-peak). This paper extends the analysis presented in [9] by using historical data of the sea state and power system operation for an entire year and considering different power system operating states as a function of the frequency (normal, alert, emergency), as established in the Spanish Grid Code on the operation of insular power systems [18].

Although there exist some potential solutions to mitigate the negative effects of wave power generation on the system frequency [19]; such as: advanced control strategies may contribute to smooth the output power of WECs [20]; and proper planning of the number of WECs and their relative position can reduce total power oscillation injected in the power system [21], we have chosen to focus on energy storage to mitigate the impact of wave power generation on the system frequency [22] since it has been already used to compensate active power oscillations of photovoltaic and wind power plants[23][24]and we think it has a great potential for this particular application [25].

The paper aims at estimating the impact caused by power generation on the frequency of an isolated small power system, analysing the contribution of energy storage to mitigate it. A methodology is presented to determine the power and energy requirements for the energy storage system, to eliminate a certain amount of frequency excursions. Moreover, interesting conclusions are drawn as regards the most suitable energy storage technologies for this particular application.

The paper is organized as follows. Section 2 presents a summary of the current European and Spanish regulations establishing criteria to determine the state of the power system as a function of the frequency. Section 3 describes the models and methodology used for the analysis. Section 4 includes a detailed study for a complete year of the power produced by wave energy park installed in a certain sea location and frequency deviations produced in the grid of the island. In addition study the convenience of the installation energy storage systems. Section 5 summarises the main conclusions of the paper.

2 Grid Codes

In this section we are presenting the most relevant present regulations related to the stability of the grid frequency, our study variable. The aim of the study of the regulations is to make known the procedures and limit values for the stability of weak and isolated electrical systems, as is the case presented in this paper.

In Europe, operational security limits for the electricity transmission system operation are established in [26], where three different system operating states are defined as a function of the system frequency for the various synchronous areas operating within Europe (Continental Europe, Great Britain, Nordic, Ireland and Northern Ireland, and Baltic), namely: normal, alert and emergency. Prior to the recent entry into force of [26], frequency limits for the Continental Europe synchronous are were found in the well-known UCTE Operation Handbook [27]. The UCTE (Union for the Co-ordination of Transmission of Electricity) coordinated the operation and development of the electricity transmission grid for the Continental Europe synchronous area until 2009, when all its operational tasks were transferred to the ENTSOE (European Network of Transmission System Operators for Electricity).

National electricity authorities must incorporated the operational security limits established in [26] into their respective national regulations on electricity transmission system operation. In [26], Continental European transmission power systems are said to be in a normal operating state when the frequency deviation is within the standard frequency range (±50 mHz), or the steady state frequency deviation is not larger than ±200 mHz for no longer than 5 minutes. The system is said to be in an alert state when the steady state frequency deviation is not larger than ±200 mHz, but is larger than ±100 mHz for more than 5 minutes or than ±50 mHz for more than 50 minutes. When the grid frequency does not meet the criteria for the normal and the alert states, the system is said to be an emergency state.

In Spain, the operation of the electricity transmission system is regulated in a set of operational procedures that can be found in the web page of the Spanish TSO (*Red Eléctrica de España* [28]). The operational procedures are defined both for the mainland power system (SEP) and the insular and extrapeninsular power systems (SEIE). The operational security limits of SEIE are regulated in [31]. The SEIE are said to be in a normal operating state when the frequency is between 49.85 and 50.15mHz, accepting intervals of less than five minutes with values outside the mentioned range and between 49.75 Hz and 50.25 Hz. In this paper, we assume that the system is in an alert operating state when the frequency deviation is not larger than ±250 mHz, but is larger than ±150 mHz for more than 5 minutes, and that is in an emergency state whenever the system frequency is outside the range between 49.75 Hz and 50.25 Hz.

Transmission System Operator (TSO) is responsible for ensuring that, whenever possible, the transmission system operates in a normal state by means of three main load frequency control processes [29]: frequency containment, restoration and replacement (in the Spanish electricity system). The processes are called primary, secondary and tertiary load frequency control. Considering that the generation of electric wave energy should not disturb the electrical network beyond its normal operation, frequency deviations of the grid produced by the oscillating active power of Wave Farm must be within the ranges established above, to avoid the activation of the load frequency control. In summary, regarding frequency values, the normal operating frequency for the Spanish system is 50 Hz and the electric power injection of the Wave Farm in insular power systems should prompt maximum variations of the frequency between 49.85 Hz and 50.15 Hz

3 Wave Farm Mathematical Model

In this paper, the influence of a wave farm in an isolated small power system grid is analysed. To reach this goal, a wave energy facility is assumed located in the North of Tenerife, and it is electrically connected to the Tenerife island grid. Some projects have been developed in this region [30][31][32][33] due to its significant wave energy potential [34] (within the range 20-70 kW/m).

The project characteristics are, in summary:

- Ocean waves data are obtained according to 3.1.
- Wave farm location is latitude, 28.4° N; longitude, 17° W.
- The WEC prime mover is a point absorber with a maximum peak power of 160 kW.
- The power take-off (PTO) is a direct-drive electric linear generator of 160-kW rated power.
- The wave farm consists of 15 groups of devices (WECs) with a layout of 9 rows in a triangular pattern.

The complete mathematical model consists on a Wave Farm Model -WFM-(3.2) and an Electric Grid Model -EGM- (3.3). The WFM is parameterised according to the WEC characteristics and the layout of the wave farm. Its output is the electric power profile using as input the ocean-wave resource conditions (3.1). The EGM is parameterised according to the grid characteristics (Tenerife Island Electric Grid) and for each grid state (electric power generated by conventional and renewable sources). Using as an input the electric power profile provides by the WFM, the EGM evaluate the electric frequency time-profiles. Fig. 1 shows the whole model.

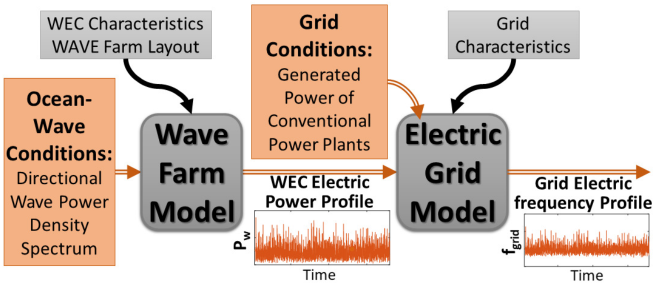

Fig. 1: Diagram Scheme of the Wave Farm Model (WFM) and Electric Grid Model (EGM) (parameters, inputs and outputs).

3.1 *Ocean Wave Resource Data*

As said above, this case study is developed for Tenerife, one of the seven main isles of The Canary Islands (Spain), in the northwest coast of Africa. Several measurement stations are available along the Archipelago, e.g., there is one at the northwest of Gran Canaria (Meteorological Buoy of Gran Canaria, reference number 2442, Fig.2 [35]). However, there are no measurement buoys around north Tenerife what implies that, to have a data set in this last island, we can take into account the numerical values computed for the, so called, SIMAR points [35], or adopting actual measured values in a nearby place, this is, the Gran Canaria buoy. That is why the comparison between both islands needs the analysis of values obtained by numerical models in two similar points.

Thus, we have proceeded to compare the SIMAR 4035011 point in the north of Gran Canaria with the SIMAR 4021014 point in the north of Tenerife. Analyzed time series goes from January 1958 to May 2017 for both cases, and has an annual range. T_p (s), peak period, and H_s (m), significant wave height, have been studied. Percentage of total events for both variables (T_p and H_s) have been used (Table 1 and 2). The values that appear in the columns of Table 1 and 2 correspond to the percentage of events for each island, the difference between the percentage of events that occurred between them (Diff) and the weighted average of those values (Weight Aver) regarding the difference (Diff) of the percentage (%) of events between the islands.The final terms correspond to the average and standard deviation of the percentage of events that occurred for each island. It also includes the sum of the difference between both and the sum of the weighted average.

As shown in Tables 1 and 2, values of peak period and significant height between the two SIMAR points differ very little. The events means for both variables are identical, and have a similar standard deviation.

IET Research Journals, pp. 1–9

Table 1 % Events Significant Height (H_s)

Hs(m)	Tenerife	Gran Canaria	Diff	Weight Aver
0.5	0.571	1.062	0.491	0.00401
1	16.227	17.559	1.332	0.225015
1.5	34.238	34.15	0.088	0.0301
2	25.886	25.709	0.177	0.04566
2.5	12.892	12.862	0.03	0.00386
3	6.001	5.47	0.531	0.0304555
3.5	2.467	2.071	0.396	0.008985
4	0.986	0.71	0.276	0.00234
4.5	0.421	0.258	0.163	0.0006
5	0.176	0.096	0.08	0.0001
5	0.135	0.053	0.082	0.00008
Average	9.090909091	9.090909091	3.646	0.35116
Stand.Dev	11.8590754	11.94886719		

Table 2 % Events Annual Peak Period (T_p)

Tp(s)	Tenerife	Gran Canaria	Diff	Weight Aver
2				
4	0.021	0.069	0.048	0.00002
6	2.607	4.243	1.636	0.056
8	26.895	28.302	1.407	0.3883
10	25.875	24.466	1.409	0.3547
12	23.257	21.637	1.62	0.3636
14	15.69	15.503	0.187	0.0292
16	4.444	4.529	0.085	0.0038
18	1.051	1.078	0.027	0.00029
20	0.141	0.153	0.012	0.00002
20	0.019	0.02	0.001	0.0000002
Average	10	10	0.6432	0.35116
Stand.Dev	11,58347323	11,2930494		

Table 3 Correlation and errors

	H_s	T_p
Pearson	0.999108	0.996368
MAE	0.351160	1.195934

The Pearson correlation coefficient and the weighted *MAE* were used as statistics and metrics [36]. MAE has been weighted by the average probability of the event for each H_s or T_p.

As we can see in Table 3, being r_{xy} so close to one and positive, it is possible to state that there is a perfect positive correlation between both data distributions for H_s and T_p. The weighted MAE between the two islands is 0.35% in wave height and 1.19% in peak period. Therefore, it is concluded that both coasts are comparable in terms of wave resource.

Following the methodology explained above, a general comparison between different points of numerical model SIMAR around Gran Canaria and Tenerife with the meteorological buoy of the north of Gran Canaria has been done. Fig. 2 shows that the northern coasts in both islands present high correlation values in terms of Pearson coefficient related to the marine resource characteristics. Therefore, the ocean-wave resource data used in this analysis came from the measurements of the meteorological buoy of the north of Gran Canaria. The list of the hourly wave power-density spectrum list during the year 2013 is used to reproduce the wave elevation-time profiles as inputs of the WFM. The parametric values Hs, Tp and incident angle values of these hourly directional spectrum are shown in the scatter diagram of the Fig. 6.

3.2 Wave Farm Model (WFM)

The Wave farm model is composed by; on one hand, a model of a single WEC; on the other hand; a script to calculate the total electric power output of the wave farm (P_{WEC}) from the previously mentioned WEC model and the layout of the 54 devices.

3.2.1 Wave Energy Converter (WEC): The WEC technology selected for our wave park is a two-body point absorber. The geometry of the absorber is the one proposed in [9] (a scheme with its main dimensions of the single WEC geometry is shown in Fig. 3(b)). The geometry was obtained according to the methodology presented in [37]; an optimization of WEC dimensions has been carried out through the application of a multiobjective differential evolutionary algorithm [34]. By minimizing the volume of the converter and maximizing the extraction of energy (objective function parameters) the optimum dimensions for the WEC were obtained, particularized to the PTO main characteristics and ocean-wave conditions of the locations.

On the other hand, from the WEC dimensions a model was obtained for a single WEC, restricted to the heave movement. In this model, the losses for the PTO (linear generator [38]) have been taken into account, as well as a PTO control strategy based on a Gain Schedule Scheme, as proposed proposed in [39] (which is modified to optimize the electric power and takes into account the PTO force limitations). This model has been realized in a state space form from the frequency characteristics for the WEC [40].

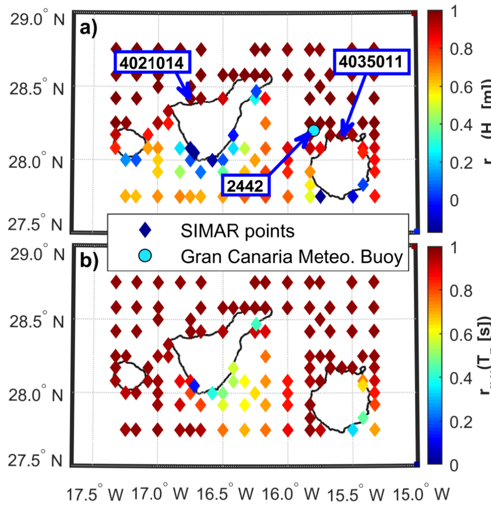

Fig. 2: Correlation (r_{xy}) value for the H_s (a) and T_p (b) values between each SIMAR point (marked with diamonds) and the Gran Canaria Meteorological Buoy (ref. number 2442, marked with a circle).Obtained from Puertos del Estado web page [35])

3.2.2 Wave Farm (WF): The wave farm considered is parameterized with layout of the total number of WEC considered. From the information of the influence of different wave farm layouts of [9], a layout of 9 rows (with a traditional triangle pattern) has been selected in order to minimize oscillation amplitude in the electric power output. In addition, based in the same study and with the same purpose, the year averaged ocean wave direction [35] of the location form an angle of 45° with the main direction of the wave farm layout. The Fig. 3(c) shows the WEC farm spatial layout, remarking the main direction of the wave farm layout, this year averaged ocean wave direction and, for sake of example, the wave direction of one simulation of the wave farm. To evaluate the output power we have applied the state space model in the time domain for the total of converters, calculating the wave elevation time-profile in each WEC spatial position, according to the selected layout (for sake of example, Fig. 3(a) shows the output power profile of a single WEC). The wave elevations time-space profile is calculated for each ocean wave conditions (3.1) from the hourly data of the wave power-density spectrums, and taking into account a multidirectional spectrum according to [41]. In order to neglect the hydrodynamic interactions between the WECs, a separation distance between them of 600m [42].

3.3 Electrical Grid

3.3.1 Grid Model: A single-bus inertial simulation model (1) has been used for the above-mentioned purposes Fig. 4. The model

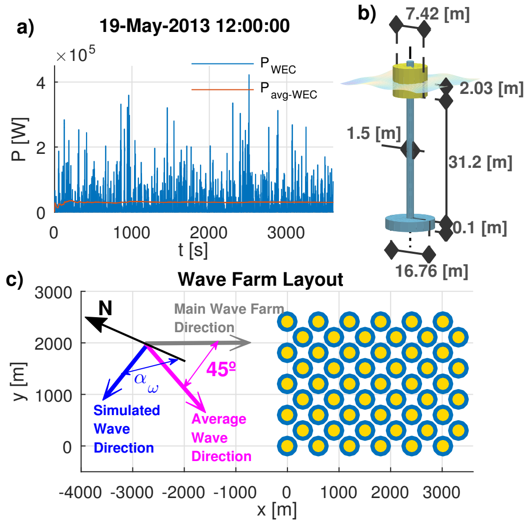

Fig. 3: a) Single WEC generated-power profile. b) Single WEC geometry scheme. c) Wave Farm Layout (including ocean wave propagation directions).

computes the system frequency deviation (f_{grid}) as a function of the variation of both the load P_{Load} and the active power injected by the WECs P_{WEC}.

The response of the primary load-frequency control of the spinning units R_1 is calculated by (2), where R represents the aggregate speed droop of all spinning generating units. The frequency insensitivity of the speed governors is considered as a small delay (T_{R1}) in the response of the primary load-frequency control.

In Tenerife power system, an automatic generation control (AGC) system is in charge of restoring the system frequency to its nominal value (50 Hz) after the performance of the primary load-frequency control. The AGC system generates an aggregate power set-point signal P_{sp} for the spinning generating units by means of a proportional-integral control loop (3). The proportional gain K_f is conceptually similar to the K-factor used in Continental European power systems [27]. A small delay is considered in the generation of the power set-point signal T_{R2}.

As can be seen in Fig. 4, the aggregate power set-point signal P_{sp} is passed through a dead band and a rate limiter. The output of the rate limiter P^*_{sp} is then used as input of a second-order linear transfer function whose output is the response of the secondary load frequency control of the spinning generating units R_2 (4) [43]. The transfer function depends on the parameter T_{sc} which has no direct physical meaning and that is proposed in [43] to properly capture the response speed of the secondary load frequency control of the spinning generating units.

The sensitivity of the load to variations in the system frequency [44], which provides a self-regulating effect, has been considered through D_{net}.

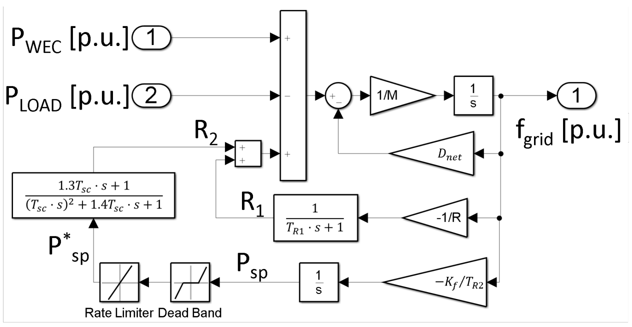

Fig. 4: Block diagram of the single-bus inertial simulation model.

The aggregate mechanical inertia M (equal 2 times the inertia constant -H-) of all spinning generating units and the aggregate speed droop (R) have been estimated as suggested in [45] and [9], from system frequency records provided by the former Transmission System Operator. The other model parameters were estimated by simulations [46].

$$M\frac{df_{grid}}{dt} = P_{WEC} - P_{Load} - D_{net}f_{grid} + R_1 + R_2 \quad (1)$$

$$\frac{dR_1}{dt} = \frac{1}{T_{R1}}\left(-\frac{f_{grid}}{R} - R_1\right) \quad (2)$$

$$\frac{dP_{sp}}{dt} = -\frac{K_f}{T_{R2}}f_{grid} \quad (3)$$

$$1.3T_{SC}\frac{dP^*_{sp}}{dt} + P^*_{sp} = T^2_{sc}\frac{d^2R_2}{dt^2} + 2\cdot 0.7T_{sc}\frac{dR_2}{dt} + R_2 \quad (4)$$

3.3.2 Electric Grid Data: The parameters of the electrical system that have been used to carry out our analysis are the data of generation (conventional and renewable) and consumption of the island of Tenerife of the year 2013. The list of the hourly generation and consumption data has been obtained from *Red Eléctrica de España* webpage [47]. These values are used to parameterise the EGM and are shown in the scatter diagram of the Fig. 6.

The renewable generation of the island (mainly solar, but with presence of wind energy) has not contribution to the inertia of the system (due to it injects to the network by means of power electronics) and the wave energy generation has the same particularity. Assuming that the wave energy generation has priority over the conventional generation in covering the electricity demand, the hourly value of the conventional generated power will be reduced in the averaged value of the wave energy power injected (P_w). Therefore, the wave energy generation introduces an oscillatory power and, in addition, reduce the inertia constant of each hourly scenario due to substitute conventional energy generation which effectively contribute to the aggregate mechanical inertia.

4 Simulation results and discussion

4.1 Simulation results

Taking into account the resource data of 3.1, and using the Wave Farm Model (WFM) described in 3.2, the hourly WEC power generated-time profiles (P_{WEC}) for the 54 WEC devices and during a complete year have been obtained. Next, each power profile is injected into the EGM described in subsection 3.3 (a balancing model or single-bus inertial model of Tenerife Island [9]), obtaining the frequency profiles (f_{grid}) hourly calculated along a complete year. The balancing model considers the state of the grid in each hour. For sake of example, a representation of these two profiles of a particular hour is showed in Fig. 5.

These profiles are obtained from the WEC farm model according to the wave characteristic (H_s, T_p and main incident angle - α_w -) and the Tenerife balancing model according to the grid state (power generated in conventional power plants, $Pgrid - cnv$). Each hourly profile of P_{WEC} and $fgrid$ are obtained according to the hourly values of this four parameters provided by *Puertos del Estado* [35] and REE [47]. Different scatter diagrams are presented in Fig. 6, crossing the variables related to the sea state (H_s, T_p and α_ω) and the variable related to the electric grid (conventional generation power) to each other. The main incident angle (α_ω) is defined as the angle between the north direction and the direction from the waves come. The representation of the different combinations demonstrate the dispersion of data. Therefore, the complete year must be analised to get conclusions. On the other hand, the graphs at the diagonal represent the histograms of the four variables.

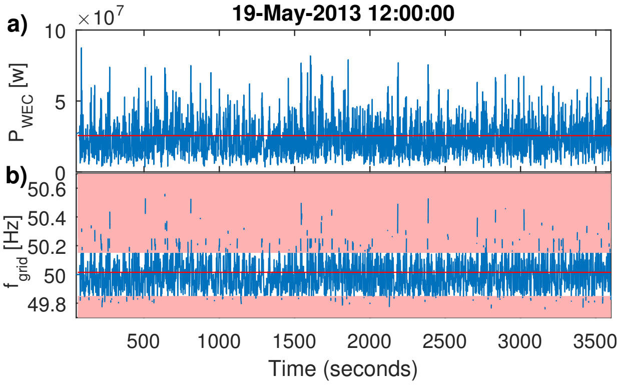

Fig. 5: a) WEC farm generated-power profile. b) System frequency profile.

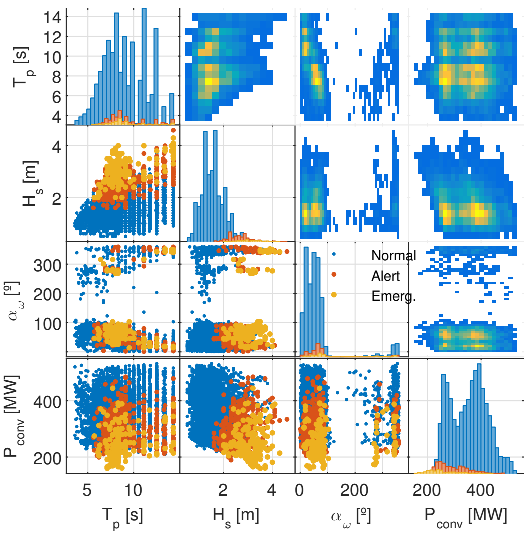

Fig. 6: The scatter diagram of the four parameters combination (H_s, T_p, α_w, $P_{grid-cnv}$) which defines each hourly case analysed in this paper (2013)

4.2 *Electric grid impact analysis*

Each hourly P_{WEC} and f_{grid} profile is analysed in order to obtain its hourly average value and variance. In addition, each peak in the power and frequency is identified. Finally, the number of alert events in each hour on which the frequency excursions overpass the normal operation limits and alert limit frequency (and the grid enter in the alert state) and the number of emergency events in each hour in which the frequency excursions overpass the alert operation frequency limits (and the grid enter in the emergency state) are evaluated (50.15 Hz and 50.25 Hz respectively, according to the Island Spanish Grid Code [18]). These two types of events are called, "alert events" and "emergency events", respectively". In addition, the total duration of these type of events is obtained. This information is used in Fig. 6, where each hourly case is shown, remarking with yellow and red points the cases where any event out of normal or alert operation frequency limits (respectively) have occurred. This information permits to confirm that the cases most susceptible to present grid frequency problems are off-peak hours with high penetration of wave energy (high H_s and T_p, which means high power waves and leads to high wave energy generation).

This graph is useful to detect how many alert and emergency cases (out of frequency limits) are produced in a year. In addition, the histogram of the instantaneous values of frequency is shown in Fig. 7(a) in order to show the percentage of time that the frequency exceeds the limit stablished by the grid codes. Although different representations could be used to analyse the frequency excursions and quantify the negative effects in the grid, a histogram for the peak values of each individual oscillations of frequency are presented in Fig. 7(b).

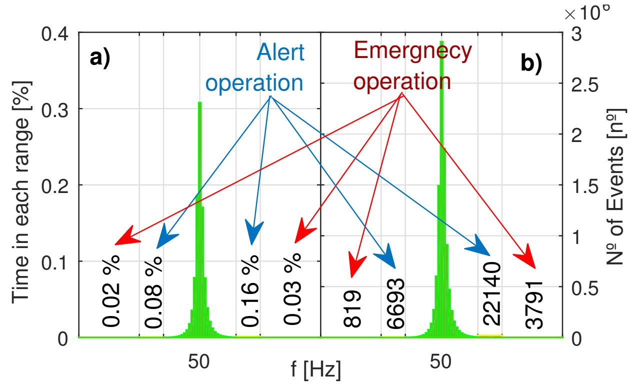

Fig. 7: a) Histogram of the instantaneous values of the frequency. b) Histogram of the peak values of the frequency excursions.

Fig. 7 showns that the wave farm connected to the Tenerife Island grid, prompts inacceptable frequency excursions. Frequency values out of the normal operation limits (frequency deviations greater than 150 mHz) appear, but these alert events are not maintained during more than 5 minutes due to the wave oscillation periods have values of 5s-25s approx. However, it would be desirable that the electric power systems remain in a normal operation state during the wave power generation. In addition, emergency events (frequency deviations greater than 250 mHz) occur too. It is worth mentioning that these unacceptable frequency excursions are caused by a wave farm with an average power penetration (relationship of instantaneous power of the wave energy and the synchronised power of the conventional power plants) of 4.02%, and with a power penetration equal or greater than 21.2% during 0.5% of the time.

Fig. 8 shows the relationship between the oscillatory power generated by the wave farm and injected into the grid, and the frequency deviations. Fig. 8(a) provides information about which is the limit of variance in power generation when it is required to take measures to compensate the power oscillations because they make the system operate outside the normal or alert operating states. Fig. 8(b) gives information about the number of alert and emergency events. Cases are grouped according to the value of the grid inertia (H_{grid}), parameter related with the robustness of the grid against frequency deviations.

Fig. 8(a) shows the linear regression of variances of P_{WEC} and f_{grid} (evaluated in each hourly simulation) for each considered H_{grid}. Fig. 8(a) obtaining goodness of fit or coefficient R^2 close to one (which leads to a good linear representation). The same representation P_{WEC} and f_{grid} variances, but grouped by the existence of out of normal and alert operation events, shows clear differentiated areas, indicated with yellow and red outline polygons in Fig. 8(a). An ANOVA test of variance [48] proves that these three groups of simulation cases (with alert events, with emergency events and with all the frequency oscillations within the normal limits, 49.85-50.15 Hz) cases come from populations whose means differ.

Due to the direct relationship between the variance of P_{WEC} and f_{grid}, the reduction of the values of the first parameter also leads to a reduction of the values of the second.

Fig. 9 shows the histogram of the variance of P_{WEC} in the simulation cases where alert or emergency events occur. The cumulative distribution function provides information about relationship between the variance of P_{WEC} and the cases of alert and emergency (unacceptable cases). The relationship between the variance of P_{WEC} and the cases of alert and emergency is direct. As the variance of P_{WEC} increases, there is an increase in alert and emergency cases. Therefore, the adequate range of operation will be the one whose variance of P_{WEC} is as small as possible, but considering the values of the Fig. 9 in order to reduce P_{WEC}

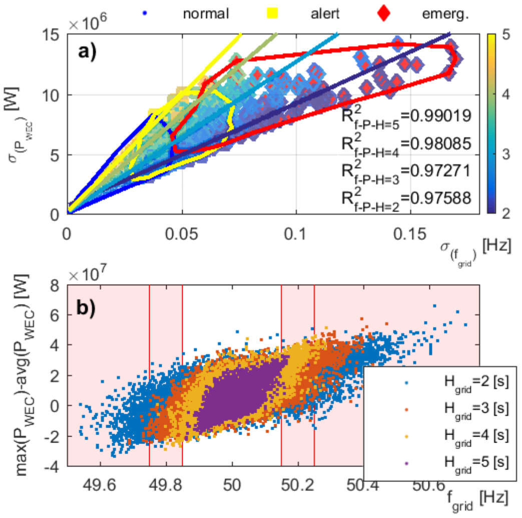

Fig. 8: a) Scatter diagram of the peaks of the P_{WEC} and f_{grid} time profiles. b) Scatter diagram of the variance of the P_{WEC} and f_{grid} time profiles, remarking the cases where alert of emergency events occurs.

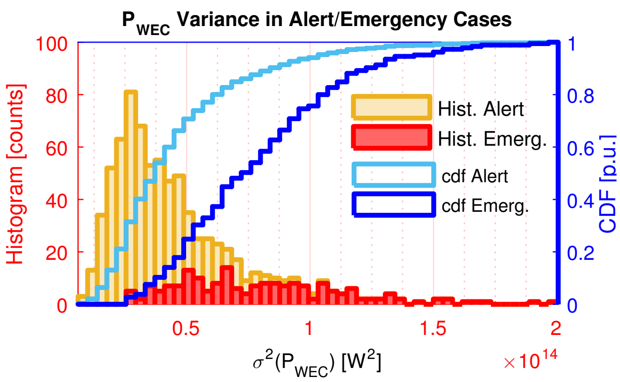

Fig. 9: Histogram of the variance of the P_{WEC} for the simulation cases with unacceptable frequency excursions

variance just to the necessary value to reduce the alert and emergency cases to a required value.

4.3 Preliminary analysis of mitigation solutions: Energy storage

From the results shown in Section 4.2, it is required to take corrective measures. One could be the curtailment of power generation but that is not convenient and would be only applied when other options are not available. Second is to act over control algorithms of generation sources but they do not provide much range of actuation. The most suitable measure to compensate the negative effects of wave generation on the system frequency is to smooth wave power oscillations by using energy storage systems (ESS), as it is shown in Fig. 10.

The ESS smooths the power injected in the grid by the wave farm. This can be achieved by absorbing the exceeding wave energy when the instantaneous wave power is above the average wave power, so that it is delivered back to the power system when the instantaneous power is below the average [49]. The average power (P^*_{smooth}) can be calculated by means of a Moving Average Filter (MAF [36]) according to (5), with a specific (windows size, WS). Considering ideal ESS, the power injected in the grid would be always equal to the average power calculated by the MAF. According to the variance properties, it is possible to find a relationship between the variance of the WEC generated power, the variance of the power injected in the grid (power smoothed by the ESS, P^*_{smooth}) and the window size of the MAF, as it is shown in (6).

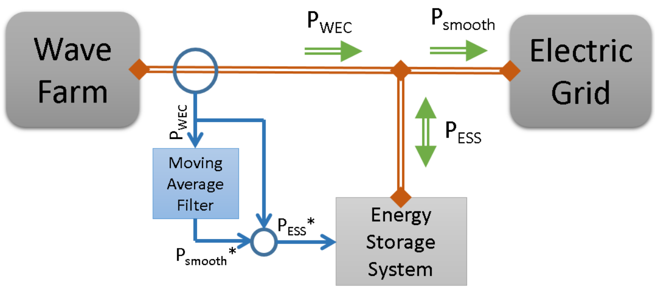

Fig. 10: Scheme of the smoothing by storage of energy

$$P^*_{smooth}(t) = \sum_{k=1}^{\frac{WS}{\Delta t}} \frac{1}{(\frac{WS}{\Delta t})} \cdot P_{WEC}(t-(k-1)\cdot\Delta t) \quad (5)$$

$$\sigma^2(P_{smooth}) = \sum_{k=1}^{\frac{WS}{\Delta t}} \sum_{j=1}^{\frac{WS}{\Delta t}} conv(P_{WEC}(t-(k-1)\cdot\Delta t), \; P_{WEC}(t-(j-1)\cdot\Delta t)) \quad (6)$$

For sake of example, the full number of non acceptable cases cannot be considered for the dimensioning of the energy storage. That would lead to an oversized ESS. For sake of example, we state the criteria is to eliminate the 80% of alert events and the 100% of emergency events (by the assumption that this variable, or a related variable, will be regulated in grid codes in a future wave energy development stages). According to this maximum limit, it is possible to analyse the minimum windows size of the MAF in each simulation case by means of Fig. 11(b), assuming the high correlation between the variances of P_{WEC} and f_{grid}.

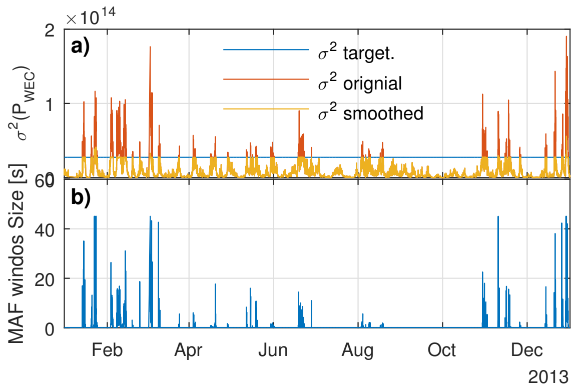

Fig. 11: a) P_{WEC} variance of the smoothed and non-smoothed simulations cases. b) MAF windows size used for smoothing P_{WEC}.

Despite it could be possible to develop a control algorithm to adapt the WS to the ocean-wave and grid state, in this paper it has been chosen a fixed WS value equal to 30s (according to Fig. 12, this value ensures to reduce the 96,5% of the hourly simulation cases). Re-analysing all the hourly simulation cases, the Fig. 13, shows the peaks frequency histogram of the smoothed power (Fig. 7(b)). The number of hourly simulation cases with emergency events are reduced to 0, and with alert events are reduced from 28833 to 221.

From the re-analysing each simulation case, it is obtained the power of the ESS (P_{ESS})required.The nominal power values are obtained as the maximum absolute value of the difference between the maximum and minimun values ($|P_{ESS-max}| = max(|P_{ESS-max}| - |P_{ESS-min}|)$). In addition, integrating the power profile along time, establishing the minimum value as the zero offset, it is possible to get the energy required (EESS-max). Fig. 14(a) and Fig. 14(b) graphs an example of the power and energy profiles of one hourly simulation case.

By presenting in Fig. 15 the cumulative distribution graph of power and energy, it can be obtained the percentages (%) of time or cases covered with a certain energy storage system. For instance, for the point marked at the figure, with a power of $2390W$ and energy of $4.009kWh$, almost 98% of the oscillations could be covered. This is useful to define the ESS technology required.

Anyhow, the ESS requirements for the study case presented in this work (corresponding to 9.651.044 oscillations, and therefore charge/discharge cycles) are very clear: high power, low energy and high number of cycles. This means that batteries are not suitable for this application, as the only way to make them fit is by greatly oversizing them in terms of energy, so that they can match the requirements of power and number of cycles. Batteries would result then a less cost-competitive technology.

On the other hand, fast energy storage technologies are better suited to fulfil the requirements of the present application. They include supercapacitors (SCs), flywheels [50] and superconducting magnetic energy storage (SMES).

Of those three, SMES is not an option at present due to its immaturity and cost. Supercapacitors (SCs) and flywheels are the most mature in terms of both Technology Readiness Level (TRL) and Customer Readiness Level, and they have already been proposed for power conditioning in renewable applications [50]. They are also a very energy-efficient alternative, and imply the lowest initial investment. The main advantages of flywheels over SCs are a lower temperature sensitivity, which allows to operate in more difficult environments with less cooling requirements, and the higher number of cycles (of the order of 5 million, five times the SCs ones). Besides, flywheels can be designed for a specific power and energy at the same time, since both magnitudes are not coupled as it happens with batteries and with SCs. This combination of higher lifetime and full independence between power and energy could make flywheel energy storage more cost-competitive than supercapacitors in the long term. In this sense, an aging-aware life-cycle cost analysis must be performed, as in [51]. In the case of SCs, the cost is estimated in 300 €/kW (expected 200 €/kW in 2030) while in the case of flywheels reaches 1000 €/kW (expected to be reduced but not much for 2030)[52]. It is important to notice that when the cost is bases on power, SCs result more advantageous than flywheels. However, if it is considered the cost in terms of energy (€/kWh), flywheels result more competitive, especially in the range of $10 - 50$ kWh devices.

Finally, conventional capacitors (CCs) are also a feasible alternative for those cases in which very low energy values are required, such as in the study case described in this work. Sometimes, it is even a good option to consider the combination of several technologies of storage, what is named hybrid energy storage, fulfilling better the requirements of energy and power when specific alternatives are not suitable for the levels required.

For the sake of example, a quick comparison is presented next between two commertial products one SC and one CC: the SC BMOD0063 from Maxwell Technologies (125 V, 63 F and 140 Wh with a voltage variation of 50%) and the HDMKP 900-2235 from Vishay (900 V, $2235\mu F$ and 0.19 Wh). According to Fig. 15, the most economic EES to compensate wave power oscillations during 98% of the time should have 4.0089 kWh and 2390 kW. This would imply 102 cells (10.7910 kWh/2524 kW) of SCs with a total mass and volume of 6517.8 kg and 7.11 m^3, or 21259 cells of CCs with a total mass and volume of 70.09 Tm and 58.41 m^3. Contrarily, CCs lack energy, so they are designed for 4.0089 Wh but permits till and 4.05 MW resulting in 21259 cells with 70.09 Tm and 58.41 m^3. The advantages of CCs are lower power losses and especially higher lifetime.

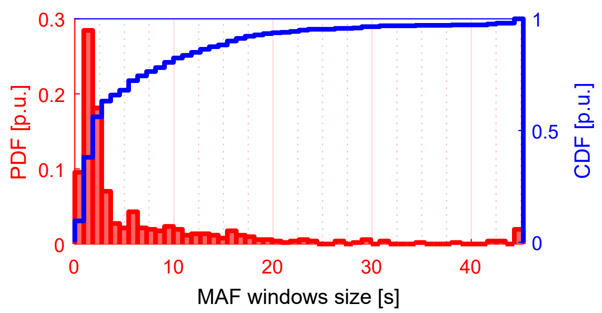

Fig. 12: Histogram of the minimum windows size to fulfil the maximum P_{WEC} variance requirements

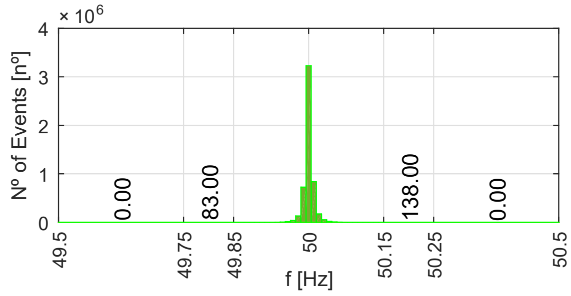

Fig. 13: Histogram of the peak values of the frequency excursions

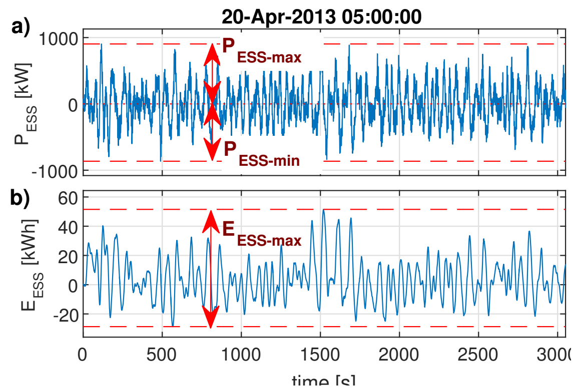

Fig. 14: a) P_{ESS} power profile b) E_{ESS} energy profile

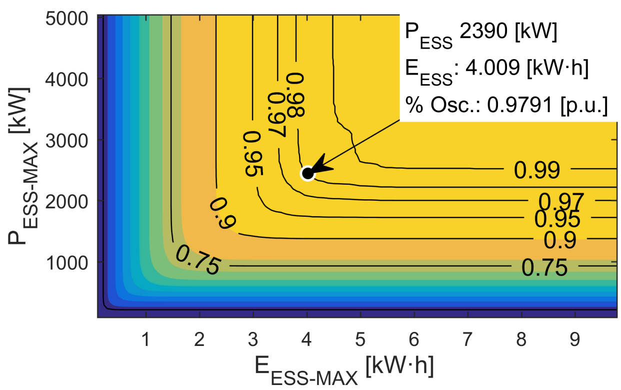

Fig. 15: Time (% of the year) in which power oscillations are completely compensated as a function of the ESS energy and power ($E_{ESS-max}$ and $P_{ESS-max}$). ESS power losses are not considered.

Although the energy and power values obtained for this particular case should not be generalized (different wave farms at different locations will imply different values), the opposite can be said regarding the number of cycles. As stated before, waves oscillate with a fundamental period between 5s and 25s, and consequently any ESS trying to compensate power oscillations will always face thousands of cycles per year. This result suggests that fast energy storage will always be needed for WEC power smoothing. For those cases in which high energy values are also required, hybrid energy storage systems should be considered.

Further work would be necessary to analyse the viability of the proposed solutions. Energy efficiency has not been taken into account in this work, but of course it should be while designing an energy-storage-based power smoothing system for wave energy applications. Fortunately, the four energy storage technologies proposed in this paper (CCs, SCs, flywheels and SMES) perform with relatively low power losses, and thus their consequences will not have a great impact in the overall design. In addition, the cost of the storage investment and the remunerations obtained from the grid operator should be considered. However, this is not possible to be considered right now since no general regulations or remuneration mechanisms have been stablished yet considering the participation of energy storage in the grid frequency control.

5 Conclusions

The paper introduces a complete methodology to analyse the effects and the corrective measures required for a wave energy farm, when being connected to a certain electric grid. The particular case of island electric grids is especially sensitive since frequency excursions beyond the security limits are detected.

The methodology requires wave data from the location to study, a simple node model of the connection grid and a model of the wave farm.

Based on these inputs, the frequency evolution of the system during a complete year is analysed and the number of unacceptable events is calculated, stating how reliable the installation of a wave energy farm is in the location of study. The procedure finally gets, taking into account some statistic considerations related to the level of confidence, the energy storage requirements in terms of power, energy and cycles.

The paper works with a particular study case to describe each stage of the method. Based on the results of a complete year analysis data, power, energy and number of oscillations are obtained. From the levels obtained, batteries are rejected as a reliable solution since the number of cycles required is too high, as well as the ratio energy/power. From the group of fast energy storage technologies, flywheels, SCs and CCs are selected and they must be considered depending on the conditions of the study case. Nevertheless, generally speaking, energy storage devices with low energy, high power and much cycles are more convenient for this application. A particular example analyses from two commercial solutions, one SC and one CC, resulting the former more appropriate for the case analysed.

References

[1] Cruz, J., : 'Ocean Wave Energy: Current Status and Future Prespectives', (Ed.): 'Springer-Verlag' (2008)

[2] Falnes, J.: 'A review of wave-energy extraction', Marine Structures.,2007, 20, pp. 185–201

[3] 'Enerdata. Global Energy Statistical Yearbook', https://yearbook.enerdata.net/world-electricity-production-map-graph-and-data.html 2014

[4] 'AquaRET, "Waves", in AquaRET Text Book', $http://www.aquaret.com/$ 2015

[5] Drew, B., Plummer, A.R., Sahinkaya,M.N : 'A review of wave energy converter technology'. Proc. Int.Mechanical Engineers,Part A : Journal of Power and Energy, 2009, pp. 887–902

[6] Seymour, J., :'The Seven Types of Power Problems - White Paper 18', 2010

[7] Falnes, J.: 'Ocean Waves and Oscillating Systems: Linear Interactions ', in Wave-Energy Extraction,(Ed.): 'Cambridge University Press', (2002, 1st edn.)

[8] Cruz, J., Sykes, R., Siddom,P., et al.:'Estimating the loads and energy yield of arrays of wave energy converters under realistic seas', Renewable Power Generation, IET., 2010, 4, (6), pp. 488–497

[9] Blanco, M., Navarro, G., Lafoz, M., Pérez, J.I.,:' Study of the impact of wave energy generation in the frequency of an island electric grid', 2017, Proceedings of the 12th European Wave and Tidal Energy Conference Ireland (EWTEC)

[10] Blavette, A., O'Sullivan, .D.L., Alcom,R., et al.:'Impact of a Medium-Size Wave Farm on Grids of Different Strength Levels', Power Systems, IEEE Transactions ., 2014, 29, (2), pp. 917–923

[11] Polinder, H., Scuotto, M., Sharma, N.D.R, et al.: 'Wave energy converters and their impact on power systems'. Future Power Systems, 2005 International Conference, 2005.

[12] Sharma, S., Huang, S.H., Sharma, N.D.R, et al.: 'System inertial frequency response estimation and impact of renewable sources in ERCOT Interconnection'.Proc. 2011 IEEE Power and Energy Society General Meeting, 2011.

[13] Kaneshiro, R.S., 'Hawaii Island (Big island) wind impact', Workshop on Active Power Control from Wind Power, 2013.

[14] Iswadi, H.R, Best, R.J., Morrow, J.: 'Irish power system primary frequency response metrics during different system non synchronous penetration'.Proc. IEEE PowerTech, 2015.

[15] Wang, Y., Silva, V., López-Botet-Zulueta,M.:'Impact of high penetration of variable renewable generation on frequency dynamics in the continental Europe interconnected system', IET Renewable Power Generation ., 2016, 10, (1), pp. 10–16

[16] Edrah, M., Anaya-Lara, O., Kockar, I., et al.: 'Impact of domestic frecuency responsive demand on the Shetland Islands network frequency stability', 2017, IET Renewable Power Generation, 24th International Conference & Exhibition on Electricity Distribution (CIRED), vol.2017, pp. 1800-1803

[17] Gill, S., Dolan M., Emhemed, A., et al.: 'Increasing renewable penetration on islanded networks through active network management: a case study from Shetland', 2015, IET Renewable Power Generation, vol. 9, no. 5, pp. 453–465

[18] REE.,'Resolución de 24 de julio de 2012, BOE 10/08/12'

[19] Lafoz, M.; Blanco, M.; Ramirez, D.: 'Grid connection for wave power farms', In Power Electronics and Applications (EPE 2011), Proceedings of the 2011-14th European Conference on; IEEE, 2011; pp. 1–10

[20] Hong, Y., Waters, R., Boström,C., et al.:'Review on electrical control strategies for wave energy converting systems', Renewable and Sustainable Energy Reviews, 2014, 31, pp. 329–342

[21] Göterman, M., Engström, J., Eriksson,M., et al.:'Methods of reducing power fluctuations in wave energy parks', Renew. Sustain. Energy., 2014, 6, (4), pp. 043103

[22] Moreno-Torres, P.; Blanco, M.; Navarro, G.; Lafoz, M.: 'Power Smoothing System for Wave Energy Converters by means of a Supercapacitor-based Energy Storage System', In 17th European Conference on Power Electronics and Applications (EPE'15-ECCE Europe); Geneva, 2015.

[23] Singh, R.,; Bansal, R.C.:'Review of HRESs based on storage options, system architecture and optimisation criteria and methodologies', 2018, IET Renewable Power Generation, vol.12, no. 7, pp–747-760

[24] Alsayed, M., Cacciato, M., Scarcella,G.:'Multicriteria Optimal Sizing of Photovoltaic-Wind Turbine Grid Connected Systems', 2013, IET Renewable Power Generation, vol.28, no. 2, pp–370-370

[25] Zhou, Z., Benbouzid, M., Fréderic Charpentier, J., et al.:'A review of energy storage technologies for marine current energy systems', Renewable and Sustainable Energy Reviews., 2013, 18, pp. 390–400

[26] 'System Operation Guideline (provisional final draft', European Comission (EC), 2016.

[27] ENTSO-E.,'Continental Europe Operation Handbook', 2004

[28] REE.,'Red eléctrica España' $http://www.ree.es/es$

[29] European Comission (EC)., System Operation Guideline (provisional final draft)

[30] Harris, M.: 'Officials sign agreement for Canary Islands wave power development', http://www.hydroworld.com/articles/2014/02/officials-sign-agreement-for-canary-islands-wave-power-development.html

[31] Veigas, M., Iglesias, G.: 'A Hybrid Wave-Wind Offshore Farm for an Island', 2014, International Journal of Green Energy, vol. 12, no. 6, pp. 570–576

[32] Veigas, M., Ramos, V., Iglesias, G.: 'A wave farm for an island: Detailed effects on the nearshore wave climate', 2014, Energy(Oxford), vol. 69, pp. 801–812

[33] Veigas, M., Iglesias, G.: 'Potentials of a hybrid offshore farm for the island of Fuerteventura', 2014, Energy conversion and management, vol. 86, pp–300-308

[34] Veigas, M., Iglesias, G.: 'Wave and offshore wind potential for the island of Tenerife', Energy Convers. Manag., 2013, 76, pp. 738–745 2016

[35] 'Prediccion de oleaje, nivel del mar ; Boyas y mareografos - Puertos del Estado', http://www.puertos.es/es-es/oceanografia/Paginas/portus.aspx, accessed 26 December 2017

[36] Willmott, C., Matsuura, K.: 'Advantages of the mean absolute error (MAE) over the root mean square error (RMSE) in assessing average model performance', Climate Research, 2005, 30, pp. 79–82

[37] REE., 'Instalaciones conectadas a la red de transporte y equipo generador: requisitos mínimos de diseño, equipamiento, funcionamiento, puesta en servicio y seguridad', 2015

[38] Santos, M., Garcí-Tabarés, L., Blanco, M., et al.: 'Testing of a full-scale PTO based on a swithed reluctance linear generator for wave energy conversion',2012, 4rd International Conference Ocean Energy (ICOE)

[39] Hals, J., Falnes, J., Moan, T.,: 'A Comparison of Selected Strategies for Adaptive Control of Wave Energy Converters', J. Offshore Mech. Arct. Eng., 2011, vol. 133, pp. 31101

[40] Yu, Z., Falnes. J., 'State-space modelling of a vertical cylinder in heave',: Appl. Ocean Res. 1995, 17, pp. 265–275

[41] Draycott, S., et al.: 'Re-creation of site-specific multi-directional waves with non-collinear current', Ocean Eng., Oct. 2017

[42] Babarit, A.,: 'A Review of the Park Effect in Arrays of Wave Energy Converters',2012, International Conference on Ocean Energy Ireland (ICOE)

[43] Egido, I., Fernández-Bernal, F., Rouco, L., et al.: 'Modelling of thermal generating units for automatic generation control purposes', 2004, IEEE Transactions on Control Systems Technology, vol. 12 (1), pp. 205–210, 2004

[44] UCTE, (Union for the Co-ordination of Transmission of Electricity). Operation handbook.(Union for the Co-ordination of Transmission of Electricity). P1 Policy 1: Load-frequency control and performance. Version 3.0, Level C, dated 12.03.2009

[45] Inoue, T., Taniguchi, H., Y. Ikeguchi, Y., et al.: 'Estimation of power system inertia constant and capacity of spinning-reserve support generators using measured frequency transients', IEEE Transactions on Power Systems, 1997, vol. 12 (1), pp. 136–143

[46] Wall, P., González-Longatt, F., Terzija, V., 'Demonstration of an inertia constant estimation through simulation', in Proc. 2010 Universities Power Engineering Conference

[47] ENTSOE.,' Continental Europe Operation Handbook', 2004

[48] Spiegel, R., Schiller, J., Srinivasan, R.A.,: 'Análisis de la varianza', Probabilidad y Estadística Schaum's Outline of Theory and Problems of Probability and Statistics. Schaum (2ed), McGraw-Hill, pp. 335–371. ISBN 978-970-10-4231-1

[49] Lafoz, M., Pasquotto, M., Moreno-Torres, P., et al.:'Reduction of power oscillations combining energy storage with prediction techniques', 2017, Conference: Proceedings of the Twelfth European Wave and Tidal Energy Conference, Cork, Ireland

[50] Chang, X., Li, Y., Zhang, W., et al.: 'Active Disturbance Rejection Control for a Flywheel Energy Storage System', 2015, Industrial Electronics, IEEE Transactions on, vol. 62, no. 2. pp. 991–1001

[51] Kovaltchouk, T., Multon, B., Ben Ahmed, H., et al.: 'Enhanced Aging Model for Supercapacitors Taking Into Account Power Cycling: Application to the Sizing of an Energy Storage System in a Direct Wave Energy Converter', 2015, Industry Applications, IEEE Transactions on, vol. 51, no. 3. pp. 2405–2414

[52] 'European Energy Storage Technology Development Roadmap', European Energy Research Alliance (EASE/EERA), $https://eera-es.eu/wp-content/uploads/2016/03/EASE-EERA-Storage-Technology-Development-Roadmap-2017-HR.pdf$